JPET Fast Forward. Published on April 27, 2007 as DOI: 10.1124/jpet.106.118034
This article has not been copyedited and formatted. The final version may differ from this version.
JPET Fast Forward. Published on April 27, 2007 as DOI: 10.1124/jpet.106.118034

JPET :#118034

## Title page:

# Neuroprotection by small molecule activators of the NGF receptor

**Bo Lin, Michael C. Pirrung, Liu Deng, Zhitao Li, Yufa Liu and Nicholas J.G. Webster**

*Veteran's Medical Research Foundation and VASDHS, San Diego, California, United States, 92161 (B.L., N.J.G.W.), the Department of Medicine, University of California, San Diego, La Jolla, California, United States 292093 (N.J.G.W.) and the Department of Chemistry, University of California, Riverside, California, United States, 92697 (M.C.P., L.D., Z.L., Y.L.).*

Downloaded from jpet.aspetjournals.org at ASPET Journals on April 16, 2024



Copyright 2007 by the American Society for Pharmacology and Experimental Therapeutics.

JPET Fast Forward. Published on April 27, 2007 as DOI: 10.1124/jpet.106.118034
This article has not been copyedited and formatted. The final version may differ from this version.



## Running title page:

a. Running title: Neuroprotection by small molecule NGF activators.

b. Corresponding author: Nicholas J.G. Webster, Ph.D, Stein Clinical Research Bldg. 201, Department of Medicine (0673), University of California, San Diego9500 Gilman Drive, La Jolla, CA 92093-0673 Tel: (858) 534-6275 FAX: (858) 534-6653 E-mail: nwebster@ucsd.edu

c. Number of text pages: 40

Number of tables: 0

Number of figures: 7

Numbers of references: 37

Number of words in the Abstract: 247

Number of words in the Introduction: 597

Number of words in the Discussion: 795

d. Abbreviations: DAQ-B1: demethylasterriquinone-B1; NGF: Nerve growth factor; QSAR: Quantitative Structure Activity Relationship; DMEM: Dulbecco's modified Eagle's medium; $IC_{50}$: represents the concentration of a drug that is required for 50% inhibition in vitro; ELISA: Enzyme-Linked ImmunoSorbent Assay; MTS: 3-(4,5-dimethylthiazol-2-yl)-5-(3-carboxymethoxyphenyl)-2-(4-sulfophenyl)-2H-tetrazolium, inner salt; IR: insulin receptor; IGF1R: Insulin-Like Growth Factor-1 Receptor.

e. Recommended Section assignment: Cellular and Molecular



Downloaded from jpet.aspetjournals.org at ASPET Journals on April 16, 2024

JPET Fast Forward. Published on April 27, 2007 as DOI: 10.1124/jpet.106.118034
This article has not been copyedited and formatted. The final version may differ from this version.



**Abstract** There is a great deal of interest in neurotrophin therapy to prevent neuronal degeneration. However, the blood brain barrier presents a major hurdle in the use of peptide therapeutics. The goal of this study was to identify small molecule, cell permeable NGF activators. Combinatorial libraries of asterriquinones (>300) and mono-indolyl-quinones (>60) were screened using a 96-well ELISA assay that detects phosphorylated TrkA, the NGF receptor. The libraries were also screened for dose-dependent cytotoxicity. From these screens, we generated QSAR models for activity and toxicity then selected two compounds 1H5 and 5E5 for further study based on high activity and low toxicity. Compound 1H5 (30 μM) is an asterriquinone that is a moderate TrkA activator (50% the activity of 100 ng/ml NGF) and shows little toxicity at concentrations up to 100 μM. 1H5 can protect differentiated PC12 neurons from apoptotic cell death induced by NGF withdrawal. Compound 5E5 (30 μM) is a mono-indolyl-quinone that is a very strong activator of TrkA (>200% the activity of 100 ng/ml NGF) and is non-toxic at concentrations up to 10 μM. Activation of TrkA can be detected at 1 μM 5E5, and 3-10 μM activates TrkA and ERK as strongly as a maximal dose of NGF (100 ng/ml). A combination of a low dose of 5E5 (1 μM) with a submaximal dose of NGF (10 ng/ml) promotes neuronal differentiation of PC12 cells. These compounds represent a new class of TrkA activators that could have potential utility in the treatment of neurodegenerative diseases.

Downloaded from jpet.aspetjournals.org at ASPET Journals on April 16, 2024

JPET Fast Forward. Published on April 27, 2007 as DOI: 10.1124/jpet.106.118034
This article has not been copyedited and formatted. The final version may differ from this version.



## Introduction:

Nerve growth factor (NGF) belongs to a family of structurally related neurotrophin proteins including BDNF, NT-3 and NT-4/5 that function to support the growth and survival of many populations of neurons (Friedman et al., 1999; Kaplan et al., 2000; Patapoutian et al., 2001). NGF binds the TrkA receptor, while BDNF and NT-4/5 bind the TrkB receptor, and NT-3 primarily binds the TrkC receptor (Patapoutian et al., 2001). These Trk neurotrophin receptors are able to protect neuronal cells from apoptosis and can stimulate neuronal regeneration in model systems (Bible and Barde, 2000; Thoenen , 2000; Huang and Reichardt, 2001; Poo , 2001). Hence, there is a great deal of interest in whether NGF and other neurotrophins can prevent or reverse cognitive decline, neuro-degenerative diseases, or promote spinal cord repair (Winkler et al., 1998; Horner and Gage, 2000). A complication is that neurotrophins also bind to the p75NTR, a member of the tumor necrosis factor (TNF) receptor superfamily (Bothwell, 1995; Dechant and Barde, 2002). Activation of the p75NTR causes cell death rather than survival and p75NTR-/- mice show reductions in neuronal cell death after pilocarpine-induced seizures compared to wild-type mice (Troy et al., 2002). Therefore, the final effect of a neurotrophin is a balance between the cell survival signal derived from the Trk receptor family and the cell death signal from the p75NTR. Indeed, each neurotrophin causes cell-death in the ~30% of cultured hippocampal neurons expressing p75 but lacking the cognate Trk receptor (Friedman, 2000).

Preclinical and clinical findings suggest that neurotrophins are a promising therapy

Downloaded from jpet.aspetjournals.org at ASPET Journals on April 16, 2024

JPET Fast Forward. Published on April 27, 2007 as DOI: 10.1124/jpet.106.118034
This article has not been copyedited and formatted. The final version may differ from this version.



for peripheral neuropathies (McMahon and Priestly, 1995) and neurodegenerative diseases, such as Alzheimer's (Sivanathan 2005; Tuszynski et al.2005) and Parkinson's disease (Shimoke and Chiba, 2001). However, neurotrophins do not make good drug candidates due to their poor pharmacokinetic behaviour and bioavailability at the desired targets. One of the major hurdles for neurotrophin therapy is the lack of passage of peptide hormones across the blood-brain barrier (Thorne and Frey, 2001;Miller , 2002). Peripheral administration of peptide hormones only leads to a small increase in their intra-cerebral concentration. This has necessitated complicated methods of delivery such as via the olfactory neural pathway (Chen et al., 1998), ex-vivo gene therapy by intracranial injection of NGF-expressing fibroblasts (Tuszynski et al., 2002), or placement of in-dwelling catheters to allow neurotrophin infusion. Therefore, much effort has been devoted to the search for non-peptidyl small molecule neurotrophin mimics, which elicit the desired neuroregenerative responses of neurotrophins (Saragovi and Gehring, 2000; Dago et al., 2002).

Asterriquinones are naturally occurring bis-indolyl-dihydroxyquinones that activate tyrosine kinase receptors. They were originally identified as activators of the insulin receptor (Zhang et al., 1999; Liu et al., 2000). The molecules are small and readily cell-permeable, and act directly on the receptor tyrosine kinase domain, although the mechanism is not known (Zhang et al, 1999). The original compound demethylasterriquinone-B1 (DAQ-B1) was demonstrated to cross the blood brain barrier and, in a separate study, shown to activate the NGF receptor, although it was toxic to



Downloaded from jpet.aspetjournals.org at ASPET Journals on April 16, 2024

JPET Fast Forward. Published on April 27, 2007 as DOI: 10.1124/jpet.106.118034
This article has not been copyedited and formatted. The final version may differ from this version.



neurons (Wilkie et al, 2001; Air et al, 2002). Therefore, we hypothesized that similar compounds could potentially activate signaling in the central nervous system and be used as oral NGF activators for neurotrophin therapy. These compounds would have the additional, very important, advantage that by targeting the kinase domain of TrkA it may be possible to avoid deleterious effects due to the activation of the p75NTR receptor, which lacks the tyrosine kinase domain. In this study, we used DAQ-B1 as a lead compound and screened a library of closely related structures to identify non-toxic and specific NGF receptor activators that have neuro-protective properties.

Downloaded from jpet.aspetjournals.org at ASPET Journals on April 16, 2024

JPET Fast Forward. Published on April 27, 2007 as DOI: 10.1124/jpet.106.118034
This article has not been copyedited and formatted. The final version may differ from this version.



## Methods:

**Materials:** Rat PC12 pheochromocytoma cells were purchased from ATCC, PC12-TrkA (clone624) cells were kindly provided by Dr. Mobley Laboratory, Stanford University Medical Center. NIH3T3-TrkA, TrkB, TrkC cells were kindly provided by Dr. Kaplan Laboratory, University of Toronto. Rabbit polyclonal anti-phospho-TrkA (Tyr490), anti-phospho-TrkA (Tyr674/675), anti-phospho-Akt (Ser473) were purchased from Cell Signaling Technology, Inc. (Beverly, MA). Rabbit anti-IR/IGF1R (pYpY1162/1163) was from Biosource (Camarillo, CA). Mouse anti-phospho-ERK (Tyr204) and rabbit polyclonal anti-TrkA (SC-11) and rabbit anti-IRβ (SC-711) and horseradish peroxidase-linked anti-rabbit or anti-mouse antibodies were purchased from Santa Cruz Biotechnology, Inc. (Santa Cruz, CA). Anti-phosphotyrosine (PY20) antibodies were from BD Transduction Laboratories (San Diego, CA). The $p13^{suc1}$ agarose conjugate was purchased from Upstate Biotechnology (Lake Placid, NY). PP1 was from Alexis Biochemical (San Diego, CA). Cell culture medium and fetal bovine and horse serum were purchased from Life Technologies (Gaithersburg, MD). 2.5S NGF was purchased from Roche (Pleasanton, CA). All other reagents were purchased from either Sigma (St. Louis, MO) or Fisher Scientific (Pittsburgh, PA).

**Cell Culture:** PC12 cells were grown in Ham's F12K medium supplemented with 5% fetal bovine serum and 15% horse serum and antibiotics at 37 °C in a 5% $CO_2$ environment. PC12-TrkA (clone624) cells were grown in DMEM (4.5 g/l glucose)



Downloaded from jpet.aspetjournals.org at ASPET Journals on April 16, 2024

JPET Fast Forward. Published on April 27, 2007 as DOI: 10.1124/jpet.106.118034
This article has not been copyedited and formatted. The final version may differ from this version.



medium supplemented with 10% fetal bovine serum and 2.5% horse serum and 200 µg/ml G-418 and antibiotics at 37 °C in a 7.5% $CO_2$ environment. CHO-TrkA (clone77) cells and CHO-IRβ cells were grown in Ham's F12 medium supplemented with 10% fetal bovine serum and 500 µg/ml G-418 and antibiotics at 37 °C in a 7.5% $CO_2$ environment. NIH3T3-TrkA, TrkB, TrkC cells were grown in DMEM (4.5 g/l glucose) medium supplemented with 10% bovine calf serum and 200 µg/ml G-418 and antibiotics at 37 °C in a 5% $CO_2$ environment.

**96-well ELISA for library screening:** CHO-TrkA cells ($1x10^4$/well) were rendered quiescent by serum starvation in Ham's F12 plus 0.1% BSA for 48 h in 96-well plates, then stimulated with compounds for 10 min at 37 $^oC$. Compounds were dissolved in DMSO and used at a final concentration of 30 µM in KRP-Hepes supplemented with 200 µg/ml ascorbic acid. Control wells received 100 ng/ml 2.5S NGF or DMSO vehicle. Each treatment was performed in triplicate. Cells were lysed with 50 µl modified RIPA buffer (30 mM Tris, pH 7.5, 150 mM NaCl, 0.5% deoxycholate, 10 mM EDTA, 0.1% SDS, 1 mM $Na_3VO_4$, 160 mM NaF, 1% triton X-100, 1 mM PMSF, 1 µM leupeptin) for 20 min and then the whole extract (50 µl) was transferred to a microtiter plate coated with anti-phosphotyrosine antibody PY20. The extract was incubated on the plate overnight at 4 °C, and then the captured proteins were washed with 0.1% Tween 20-PBS buffer three times. The immobilized proteins were probed with anti-TrkA antibodies and detected by anti-rabbit-IgG-HRP using a colorimetric assay with TMB as substrate. The data are

Downloaded from jpet.aspetjournals.org at ASPET Journals on April 16, 2024

JPET Fast Forward. Published on April 27, 2007 as DOI: 10.1124/jpet.106.118034
This article has not been copyedited and formatted. The final version may differ from this version.



presented as percent activity relative to the 100 ng/ml NGF.

**Western Blotting:** Cells ($1x10^6$/well) were starved for 48 h in 6-well plates then stimulated with compounds or NGF for 10 min, washed with ice-cold PBS, lysed with 100 µl SDS sample buffer (50 mM Tris, pH 6.8, 10% glycerol, 2% SDS, 0.005% bromophenol blue, 100 mM dithiothreitol) boiled for 10 min to denature proteins and sonicated for 15 min to shear the chromosomal DNA. Equal volumes (30 µl) of lysate were separated by SDS-PAGE on 7.5% gels, and electrotransferred to polyvinylidene difluoride (PVDF) membranes (Immobilon-P, Millipore, Bedford, MA). The membranes were blocked with 5% nonfat dried milk in TBS-Tween (50 mM Tris-HCl, pH 7.4, 150 mM NaCl, 0.1% Tween 20) for 60 min at room temperature. Blots were incubated with primary antibodies in blocking buffer overnight at 4 $^oC$, washed three times in TBS-Tween and then incubated with horseradish peroxidase-linked secondary antibodies followed by chemiluminescent detection. Anti-phospho-TrkA (Tyr490), anti-phospho-TrkA (Tyr674/675), anti-phospho-Akt (Ser473), anti-phospho-ERK1 (Tyr204), anti-phosphotyrosine (PY20) antibodies were used at a dilution of 1:1000. To verify protein loading, the PVDF membranes were immediately stripped with stripping buffer (0.5 M NaCl and 0.5 M acetic acid) for 30 min at room temperature. The membrane was then washed once for 10 min in TBS-Tween, reblocked, and blotted with antibodies to internal control protein-ERK1. The intensities of the bands were quantified using Image J with an Agfa Arcus II scanner.

Downloaded from jpet.aspetjournals.org at ASPET Journals on April 16, 2024

JPET Fast Forward. Published on April 27, 2007 as DOI: 10.1124/jpet.106.118034
This article has not been copyedited and formatted. The final version may differ from this version.



**Cell viability:** After the cells ($5x10^4$/well) were cultured for 72 h with increasing concentrations of compounds (3, 10, 30, 100 µM), the number of viable cells was determined with the MTS nonradioactive cell proliferation assay as recommended by the manufacturer (Promega, Madison, WI). Briefly, 20 µl freshly prepared MTS/PMS solution was added to each well, and the absorbance at 490 nm was recorded after incubating at 37 °C in the humidified 5% $CO_2$ chamber for 1–4 h.

**PC12 Survival assay:** Estimation of the survival of differentiated PC12 cells, deprived of serum and NGF, was carried out as described previously (Gronborg et al., 1999) with minor modifications. In brief, $1x10^4$ PC12 cells were seeded in each well of a 96-well plate and differentiated in the presence of serum and 100 ng/ml 2.5S NGF for 7 days. The medium was replaced with serum-free Ham's F12K medium supplemented with compounds at the indicated concentrations. NGF (100 ng/ml) was included as a positive control. The number of viable cells was evaluated at 24 h, 48 h and 72 h by measurement of the ability of the cells to reduce the tetrazolium compound MTS (Promega) according to instructions given by the manufacturer.

**Stimulation of neurite outgrowth in PC12 cells:** PC12 cells were seeded in poly-L-lysine-coated 6-well plates ($2x10^5$/well) in growth medium. The next day, cells were stimulated with 5E5, NGF, 5E5 plus NGF in normal medium for 4 days, changing medium with treatments every two days. For each well, approximately 10 images were



Downloaded from jpet.aspetjournals.org at ASPET Journals on April 16, 2024

JPET Fast Forward. Published on April 27, 2007 as DOI: 10.1124/jpet.106.118034
This article has not been copyedited and formatted. The final version may differ from this version.



acquired randomly by scanning the wells from left to right and top to bottom. For calculation of percent of neurite bearing cells, cells were considered to be neurite bearing when the neurite length is >1.5x cell body diameter (Morooka and Nishida, 1998). For neurite length measurements, the lengths of the individual neurites for each cell were measured using the NIH Image J software. Length was defined as the straight-line distance from the tip of the neurite to the junction between the cell body and neurite base. In the case of branched neurites, the length of the longest branch was measured from the tip of the neurite to the cell body, and then each branch was measured from the tip of the neurite to the neurite branch point (Schmidt et al., 1997). In each instance, 8 random fields (100×) were scored (total of 1500 cells) for neurite outgrowth.

**Quantitative Structure Activity Relationship (QSAR) studies:** Using the TSAR 3.0 suite of programs (Accelrys, San Diego, CA), QSAR studies were performed on the original data set of 334 molecule asterriquinone library and 62 molecule mono-indolyl-quinone library. For the asterriquinone library, 14 substituents on the core indolequinone structure of DAQ-B1 were considered (Fig. 2A). Thirteen independent variables for each substituent were incorporated into the initial QSAR model, including molecular refractivity (aromatic), verloop steric parameters (L, B1, B2, B3, B4), molecular mass, molecular surface area, molecular volume, ellipsoidal volume, MlogP, Weiner coefficient. (Kovatcheva A. et al., 2003). We also included 6 whole molecule descriptors, including molecular mass, molecular volume, ellipsoidal volume, total dipole

Downloaded from jpet.aspetjournals.org at ASPET Journals on April 16, 2024

JPET Fast Forward. Published on April 27, 2007 as DOI: 10.1124/jpet.106.118034
This article has not been copyedited and formatted. The final version may differ from this version.



moment, log P, molecular refractivity. Due to the rotational symmetry of the parent molecule (the indoles are equivalent), the library was numbered in both directions and combined. For the mono-indolyl-quinone library, 8 substituents were considered. Twenty-five initial independent variables were considered for each substituent, including PI (aromatic), MR (aromatic), Swain and Lupton F, Swain and Lupton R, Sigma Meta, Sigma Para, Taft ES, verloop steric parameters (L, B1, B2, B3, B4, B5), molecular mass, molecular surface area, molecular volume, moment of inertia (size 1,2,3; length 1,2 3), ellipsoidal volume, MlogP, and Weiner coefficient. As the monoquinone library was much smaller than the asterriquinone library, we used data reduction techniques to eliminate variables with high correlation. Correlation coefficients were generated between all potential variables. Variables with correlation coefficients greater than 0.90 were considered redundant and all but one were eliminated. This data reduction resulted in 45 variables with reduced collinearity.

Forward feed neural networks were generated using the TrkA activity or toxicity as target parameter and the substituent or whole molecule parameters as variables. The ratio of variables to samples was approximately 1:2 to prevent over-fitting of the data. After convergence of the data, the model predicted values were plotted against the empirical values and correlation coefficients generated. The best RMS fit of the model was compared to the test RMS fit to gauge the predictive value of the model. The parameter dependencies were determined by systematically varying each parameter and measuring the effect on the output variable.

Downloaded from jpet.aspetjournals.org at ASPET Journals on April 16, 2024

JPET Fast Forward. Published on April 27, 2007 as DOI: 10.1124/jpet.106.118034
This article has not been copyedited and formatted. The final version may differ from this version.



Multiple regression models were generated using F-stepping. Initially, models were limited to linear regression. Leave out groups-of-three cross validation with varied random selections was used to test predictive power ($r^2$(CV)). The F-enter and F-leave parameters were systematically varied to optimize the model without including too many parameters. Partial F-values were inspected to look for obvious cut-offs. After running linear regression models, the models were re-run but allowing the parameters to vary up to the $4^{th}$ power. The predicted values were correlated against the empirical values.

**Statistical analysis:** Biological data were analyzed by ANOVA or t-test in Microsoft Excel 2000. Results are presented as mean and standard deviation or stand error. A two-tail P value $<0.05$ was considered significant.

Downloaded from jpet.aspetjournals.org at ASPET Journals on April 16, 2024

JPET Fast Forward. Published on April 27, 2007 as DOI: 10.1124/jpet.106.118034
This article has not been copyedited and formatted. The final version may differ from this version.



## Results:

### Screening combinatorial libraries for activation of TrkA

The lead compound DAQ-B1 (2-[2-(1,1-Dimethyl-allyl)-1H-indol-3-yl]-3,6-dihydroxy-5-[7-(3-methyl-but-2-enyl)-1H-indol-3-yl]-[1,4]benzoquinone) that was identified as an activator of the insulin receptor has a pseudo-symmetrical bis-indolylquinone structure (Fig. 1A). We synthesized a library of asterriquinones using a combinatorial approach (Fig. 1B). Details of the synthetic route have been published previously ( [a]Pirrung et al, 2005). Aliphatic, aromatic and halogen substitutions were included at different positions on the indole rings and the hydroxyl of the quinone ring generating 14 possible substitution positions (Fig. 2A). This library of 334 compounds was tested for activation of the TrkA using an ELISA assay that detects phosphorylated TrkA. Briefly, all tyrosine-phosphorylated proteins were captured by PY20 antibody coated on microtiter plates. The presence of TrkA among the phosphorylated proteins was then detected by anti-TrkA antibodies. Activation of TrkA was compared to stimulation by a maximal concentration of NGF (100 ng/ml) and is presented as % NGF. In this assay, the original compound DAQ-B1 activated TrkA to 61% the effect of NGF and ninety-one other compounds had activity >25% NGF (Supporting information 1). As an index of the assay, the mean SD of the total assay for all compounds is about ±20%. This dataset was used to generate QSAR models for activation of TrkA. We derived forward feed neural networks for activation of TrkA. Thirteen parameters were considered for each of the 14 substituents as well as 6 whole

Downloaded from jpet.aspetjournals.org at ASPET Journals on April 16, 2024

JPET Fast Forward. Published on April 27, 2007 as DOI: 10.1124/jpet.106.118034
This article has not been copyedited and formatted. The final version may differ from this version.



molecule parameters, for a total of 188 variables for modeling. Initial models were unsuccessful. We suspected that the rotational symmetry of the molecule was limiting the power of the model (substituent 2 is equivalent to substituent 8, etc.), so we duplicated the library but labeled the substituents in the opposite direction and combined the two. The resulting neural net had a best RMS fit of 0.098 after 3482 cycles of training. This is very close to the test RMS fit (0.103), which indicates good predictive power. The plot of predicted TrkA activation vs. observed activation is shown (Fig. 2B). The model gave a good fit to the data ($r^2$ = 0.53) explaining 53% of the variation in activity. The model dependencies were inspected by varying each parameter in turn. Symmetrical substituents 2/8 and 6/12 contributed six of the eight top dependencies. The eight parameters that showed the greatest dependency are shown in the Supporting Information 1. The data was also modeled using multiple regression analysis. The same 188 independent variables were considered and 27 variables were included in the final linear regression model using F-test stepping (F to enter=2, F to leave=2). Cross-validation leaving out each of 10 groups in turn was performed to test predictive power. The resulting model was highly significant (Fig. 2C), showed good correlation, explained approximately 40% of the variance ($r^2$ = 0.39), and had reasonable predictive power ($r^2$ (CV) = 0.30). Non-linear regression models allowing parameters to vary up to the $4^{th}$ power did not improve the fit. The 10 most significant parameters include Verloop B4 on substituents 2/8, Verloop B1 on substituents 10/4, ellipsoidal volume of substituent 9, molecular volume on substituents 11/5, total dipole moment on substituent 3, and

Downloaded from jpet.aspetjournals.org at ASPET Journals on April 16, 2024

JPET Fast Forward. Published on April 27, 2007 as DOI: 10.1124/jpet.106.118034
This article has not been copyedited and formatted. The final version may differ from this version.



molecular mass or LogP for the whole molecule (Supporting Information 2). As expected, the regression model included similar parameters on symmetrically related positions, e.g. 2 and 8, 4 and 10, 5 and 11. The results of the modeling of asterriquinone activation data are depicted in schematic form in Figure 2D. The QSAR models suggest that substituents 2, 8 and 11 on the indole ring are critical for the ability to activate TrkA as they are found by both modeling approaches.

We also tested 62 mono-indolyl-quinone intermediates against TrkA ( [b]Pirrung et al, 2005). The generic structure is shown in Fig. 2D. Many of the mono-indolyl-quinones also activated TrkA (Supporting information 2), and we used QSAR to model the activity of the mono-indolyl-quinones. Eight positions of substitution were considered. Due to the smaller number of compounds in this library, we could not use all 200 substituent variables for the QSAR modeling. Therefore, we used a data reduction method to eliminate variables that are highly correlated resulting in 45 final variables with reduced co-linearity. The forward feed neural network model explained approximately 46% of the variance in activity ($r^2$ = 0.46) (Fig. 2E). The best RMS fit was 0.038 after 1351 cycles of training compared to the test RMS fit of 0.22 indicating reasonable predictive power. The major dependencies were analyzed. The PI on substituent 7 and molecular refractivity and $\sigma_p$ on substituent 6 showed the greatest dependencies (Supporting information 3). The data were also modeled using multiple regression analysis. The 45 independent variables were considered and 10 variables were included in the final linear regression model using F-test stepping (F to enter=1, F to leave=1).



Downloaded from jpet.aspetjournals.org at ASPET Journals on April 16, 2024

JPET Fast Forward. Published on April 27, 2007 as DOI: 10.1124/jpet.106.118034
This article has not been copyedited and formatted. The final version may differ from this version.



Cross-validation by leaving out each of 3 groups in turn was performed to test predictive power. The resulting model for TrkA activation shows a high correlation (r = 0.90) between predicted and measured activity and explains 80% of the variance in the data, and is very predictive ($r^2$(CV) = 1) (Fig. 2F). The significant individual terms include PI on substituent 7, Swain and Lupton R on substituent 5, molecular mass or Taft ES on substituents 4, and Weiner coefficient on substituent 6 (Supporting information 4). The results of the modeling of monoquinone activation data are shown in schematic form in Figure 2H. These models point to the 4, 5 and 6 substituents on the indole ring and the 7 substituent on the quinone ring being important for mono-indolyl-quinone activation of TrkA.

**Screening combinatorial libraries for toxicity**

We also measured the toxicity of the library compounds against CHO-TrkA cells using MTS nonradioactive cell proliferation assay to measure cell viability (Supporting information 1 and 2). Increasing concentrations of each compound were tested (3, 10, 30, & 100 μM). Many compounds showed a dose dependent toxicity with decreased cell viability. The four point dose response curves were used to calculate $IC_{50}$ values. Compounds that did not show dose dependent cytotoxicity over the concentration range tested were arbitrarily assigned $IC_{50}$ values of 300 μM. Activation of TrkA did not correlate with $IC_{50}$ for toxicity or cell viability at 100 μM compound demonstrating that the toxicity is not activity dependent (Fig. 3A and B).



Downloaded from jpet.aspetjournals.org at ASPET Journals on April 16, 2024

JPET Fast Forward. Published on April 27, 2007 as DOI: 10.1124/jpet.106.118034
This article has not been copyedited and formatted. The final version may differ from this version.



The cell viability data was also modeled by QSAR. The same 188 parameters were considered for the asterriquinone library as before. The resulting neural network had a best RMS fit of 0.137 after 2573 cycles of training (Fig. 3C). The model showed a good correlation between predicted and actual viability data ($r^2$ = 0.54). Analysis of the dependencies did not reveal any individual parameter that contributed dominantly to the model (data not shown). Multiple linear regression analysis generated a model containing 21 variables that explained 46% of the variance in the data with good predictive power ($r^2$ = 0.46, $r^2$(CV) = 0.37) (Fig. 3D). The results of modeling the asterriquinone cell viability data are shown schematically in Figure 3G. The most significant individual terms in this model are molecular volume of the whole molecule, ellipsoidal volume on substituents 4/10 and 6/12, Verloop L steric parameter on substituent 6/12, and aromatic molecular refractivity on substituent 2/8. According to this model, viability is favored by large volume substituents 4/10, 6/12 and 2/8 on the indole ring (Supporting information 3). These predictors are different from the predictors of TrkA activation, which depend on steric parameters, in agreement with the lack of dependency of TrkA activation and toxicity. Interestingly, substituents on the 2/8 positions also favor TrkA activation suggesting that this may provide a useful site for further structural modifications.

Similar QSAR models were generated for the mono-indolyl-quinone library using the reduced set of 45 parameters. The resulting neural network had a best RMS fit of 0.148 after 849 cycles of training and showed a good correlation ($r^2$ =0.47) (Fig. 3E).



Downloaded from jpet.aspetjournals.org at ASPET Journals on April 16, 2024

JPET Fast Forward. Published on April 27, 2007 as DOI: 10.1124/jpet.106.118034
This article has not been copyedited and formatted. The final version may differ from this version.



As we had observed for the asterriquinone library, analysis of the dependencies did not reveal any dominant variables in this model. Multiple linear regression analysis generated a model containing 14 variables and showed good predictive power ($r^2$=0.69, $r^2$(CV)=1) (Fig. 3F). The most significant individual terms in this model are PI on substituent 7, Verloop L steric parameter or Taft ES on substituent 6, $\sigma_p$ on substituent 5 (Supporting information 4). The results of modeling the monoquinone cell viability data are shown schematically in Figure 3G.

**Selection of TrkA activators and confirmation of activity.**

We selected 1H5 (2-(6-Chloro-1H-indol-3-yl)-5-(2-cyclopropyl-1H-indol-3-yl)-3,6-dihydroxy-[1,4]benzoquinone) from the asterriquinone library and another compound 5E5 (2,5-dimethoxy-3-(7-fluoro-1H-indol-3-yl)-[1,4]-benzoquinone) from the mono-indolyl-quinone library for further study based on good NGF activator activity and low toxicity. 1H5 contains a chlorine substitution on one indole group and a cyclopropyl group on the other indole (Fig. 4A). The latter group is particularly interesting as it would be predicted to force the indole and the quinone rings to be orthogonal due to steric hindrance (Fig. 4B). The monoquinone 5E5 contains a fluorine substitution at the 7-position of the indole ring and two-methoxy substitutions on the quinone ring (Fig. 4A). The 2-methoxy groups on the quinone ring increases the dihedral angle between the indole and quinone similar to the 2-substitution on the indole (Fig. 4C). The ability of these two compounds to activate TrkA is shown in Fig. 4D.



Downloaded from jpet.aspetjournals.org at ASPET Journals on April 16, 2024

JPET Fast Forward. Published on April 27, 2007 as DOI: 10.1124/jpet.106.118034
This article has not been copyedited and formatted. The final version may differ from this version.



1H5 has approximately 50% the effect of NGF whereas 5E5 has about 200% the effect of a maximal dose of NGF. The dose dependent cytotoxicity of these compounds is shown in Fig. 4E. The $IC_{50}$ for the original compound DAQ-B1 is 5 μM. The monoquinone 5E5 is less toxic with an $IC_{50}$ of 29 μM. The asterriquinone1H5 was non-toxic up to 30 μM but started to show toxicity at 100 μM.

**The asterriquinone 1H5 can protect differentiated PC12 neurons from apoptosis induced by NGF and serum withdrawal**

We used PC12 pheochromocytoma cells to test the neurotrophic properties of the selected compounds. These cells undergo NGF-dependent neuronal differentiation and the differentiated neurons require NGF for continued cell survival. The ability of the asterriquinone 1H5 to activate TrkA in these cells was confirmed by immunoblotting with antibodies to specific tyrosine phosphorylation sites. 1H5 caused a dose dependent increase in phosphorylation of tyrosine 490 on TrkA and also activated ERK and Akt downstream of the receptor (Fig. 5A). We utilized PC12 cells that stably express TrkA to maximize our ability to detect TrkA activation. The activator activity in PC12-TrkA cells (45% the activity of 100 ng/ml NGF at 30 μM) was similar to the CHO-TrkA cells used for the library screen. Similar results were obtained in the parental PC12 cells (data not shown). To determine whether activator-induced TrkA activation was capable of stimulating a neurotrophic biological response, the asterriquinone 1H5 was tested in a neuronal survival assay. Briefly, the parental PC12 cells were differentiated in complete



Downloaded from jpet.aspetjournals.org at ASPET Journals on April 16, 2024

JPET Fast Forward. Published on April 27, 2007 as DOI: 10.1124/jpet.106.118034
This article has not been copyedited and formatted. The final version may differ from this version.



medium with 100 ng/ml NGF for 7 days, and then changed to serum free medium (SFM) with or without TrkA activators. Cell viability was determined at 24 h, 48 h, 72 h using the mitochondrial dye MTS (Fig. 5B). At 72 h, viability was 31±6% in control PC12 cells, 42±5% in cells treated with 30μM 1H5, 70±4% in cells treated with 100 ng/ml NGF alone. Data are presented as percentage of the positive control cells treated with 100 ng/ml NGF in complete medium. Cell survival was not improved at 100 μM as the activators start to be cytotoxic at that dose (data not shown). Under the microscope, most of the negative control cells (SFM only) showed multiple apoptotic figures, broken cells, and cellular debris. Treatment with NGF preserved cell morphology and neurites can be seen on many cells. Treatment with activator 1H5 preserved the morphology of the cell bodies and prevented apoptotic figures, but there is a decrease in the number of neurites on the cells (Fig. 5C).

**The monoquinone 5E5 has additive effects with NGF to promote neuronal differentiation.**

The library screen indicated that 5E5 was a strong activator of TrkA in CHO-TrkA cells. Therefore, we determined the full dose response curve for activation of TrkA and downstream signaling by 5E5 in PC12-TrkA cells. Phosphorylation of TrkA on tyrosines 490 and 674/675 is observed with 1 μM 5E5 and increases according to the doses (Fig. 6A and B). Phosphorylation of ERK (Tyr204) (Fig. 6 C) and Akt (Ser473) (Fig. 6D) parallels that of the receptor demonstrating that 5E5 activates NGF signaling



Downloaded from jpet.aspetjournals.org at ASPET Journals on April 16, 2024

JPET Fast Forward. Published on April 27, 2007 as DOI: 10.1124/jpet.106.118034
This article has not been copyedited and formatted. The final version may differ from this version.



pathways leading to MAPK and PI-3Kinase activation. Maximal activation of PI-3Kinase/Akt, however, is consistently weaker with 5E5 than NGF, but ERK activation is comparable. 5E5 caused phosphorylation of FRS2/SNT, a differentiation-specific target of NGF in neurons and PC12 cells (2-fold vs. NGF) (Fig. 6E). The time course of stimulation of the TrkA receptors by 5E5 and NGF is different, however. NGF stimulation leads to the rapid and prolonged activation of TrkA phosphorylation (> 4 h); 5E5 stimulation leads to the same rapid activation of TrkA but phosphorylation decreased to basal levels over 60 min (Fig. 6F). This may have important implications for the ability of these activators to stimulate neuronal differentiation as prolonged activation of signaling is required. We also compared the specificity of activating Trk receptors in NIH3T3-TrkA or TrkB or TrkC cells. 5E5 was a weaker activator of TrkB (12% the activity of 100 ng/ml BDNF at 30 μM) or TrkC (43% the activity of 100 ng/ml NT-3 at 30 μM) receptors suggesting that 5E5 is more selective for TrkA (209% the activity of 100 ng/ml NGF at 30 μM) (Fig. 6G, H and I). Previous results have shown an indirect method for activation of the Trk receptor through Src family members that is inhibited by the Src inhibitor-PP1 (Lee and Chao, 2001). To rule out indirect activation of TrkA, PC12-Trk cells were pretreated with PP1 for 30 min, and then stimulated with 30 μM 5E5 or 100 ng/ml NGF for 10 min, or with 100 μM adenosine for 2h. Results indicated that phosphorylation of Trk receptor induced by 5E5 or NGF is insensitive to PP1 but phosphorylation induced by adenosine is blocked (Fig. 6J). Because DAQ-B1 was first identified as an insulin receptor activator, we tested the ability of our selected compounds

Downloaded from jpet.aspetjournals.org at ASPET Journals on April 16, 2024

JPET Fast Forward. Published on April 27, 2007 as DOI: 10.1124/jpet.106.118034
This article has not been copyedited and formatted. The final version may differ from this version.



to activate the insulin receptor in CHO-IRβ cells. Interestingly, asterriquinone 1H5, which is most closely related to DAQ-B1, also activated the IR, but the monoquinone 5E5 showed no ability to activate the IR (Fig. 6K).

To determine whether 5E5-induced TrkA activation was capable of stimulating a neurotrophic response, we tested the ability of 5E5 to cause neuronal differentiation. PC12 cells were stimulated with complete medium plus 100 ng/ml NGF or 10 μM 5E5 (maximal non-toxic dose) for 4 days. 5E5 was unable to support neuronal differentiation under these conditions (data not shown). We then tested whether sub-maximal doses of both NGF (10 ng/ml) and 5E5 (1 μM) could support differentiation. Neurite length was measured and percent of neurite bearing cells was calculated. As before, 5E5 alone did not support differentiation. A low dose of 10 ng/ml NGF alone was partially able to support differentiation (12% neurite positive cells) compared to a maximal dose of 100 ng/ml NGF (22% neurite positive cells). Similar effects were observed when counting the number of neurite bearing cells and the length of individual neurites (Fig. 7A and B). Addition of 1 μM 5E5 to the low dose of NGF restored maximal differentiation (Fig. 7C). These findings demonstrate that the TrkA activator can potentiate the effect of low doses of NGF and may improve neuronal differentiation.

Downloaded from jpet.aspetjournals.org at ASPET Journals on April 16, 2024

JPET Fast Forward. Published on April 27, 2007 as DOI: 10.1124/jpet.106.118034
This article has not been copyedited and formatted. The final version may differ from this version.



## Discussion:

In this study, we developed combinatorial libraries of asterriquinones and screened them against TrkA receptor. We screened 334 asterriquinones and 62 mono-indolyl-quinones and identified 27 asterriquinones and 6 mono-indolyl-quinones as TrkA activators. We developed QSAR models for activation of the TrkA receptor based on forward feed neural networks and multiple regression analysis. Both methods gave models that are predictive of TrkA activator activity; the asterriquinone models explain approximately 40-50% of the variance, and the monoquinone models explain approximately 50-80% of the variance. The difference in the explained variance may be the result of fewer possible substituents in the mono-indolyl-quinone structure (8 positions) compared to the asterriquinone structure (14 positions) as the number of possible structures increases exponentially with number of positions ($n^8$ vs. $n^{14}/2$ structures were, n is the number of possible substituents at each position). Hence, we may not have enough asterriquinones to derive better models. Models from both the asterriquinones and mono-indolyl-quinones highlight the importance of substitutions at critical residues for activation of TrkA.

Based on the current models, a bulky substituent on the 2 position of the indole favors TrkA activation and also reduces toxicity. This position is critical, as these substitutions would be expected to twist the indole group out of the plane of the quinone due to steric hindrance between the quinone oxygen and hydroxyl, and C-2 and C-4 of the indole group. Molecular modeling of C-2 substituted asterriquinones and



Downloaded from jpet.aspetjournals.org at ASPET Journals on April 16, 2024

JPET Fast Forward. Published on April 27, 2007 as DOI: 10.1124/jpet.106.118034
This article has not been copyedited and formatted. The final version may differ from this version.



mono-indolyl-quinones indicates a dihedral angle of 75-90 $^{o}$ between the quinone and indole groups (Fig. 4B and C). Dihedral angles in compounds lacking a C-2 substituent are typically 35˚ due to the smaller size of the hydrogen atom. Asterriquinones have been proposed to have cytotoxic effects due to their ability to intercalate into DNA. The ability to intercalate depends on the co-planarity of the aromatic groups, so a reasonable explanation for the decreased toxicity of 2-substituted asterriquinones is the orthogonal orientation of the indole with respect to the quinone prevents intercalation. These activity and toxicity models may thus prove useful in the design of second and third generation compounds with optimal TrkA activity and minimal toxicity.

The asterriquinone chosen for further study, 1H5, is moderate activator of TrkA, is non-toxic up to 30 μM, and can provide modest protection of PC12 cells from neurotrophin-withdrawal induced cell death. The compound provides proof-of-principle that small molecule TrkA activator can have neuroprotective effects. The mono-indolyl-quinone 5E5 was chosen for further study as it is a very strong activator of TrkA, although having a cytotoxic effect above 10 μM. This cytotoxicity prevented us from demonstrating a neuroprotective effect in the neurotrophin-withdrawal induced cell death model used for the asterriquinone. However, we were able to demonstrate that 5E5 potentiates the effect of low dose NGF to cause neuronal differentiation. This is likely related to the observation that 5E5 and NGF have additive effects on TrkA activation (Supporting information 5). This is particular appealing for therapeutic



Downloaded from jpet.aspetjournals.org at ASPET Journals on April 16, 2024

JPET Fast Forward. Published on April 27, 2007 as DOI: 10.1124/jpet.106.118034
This article has not been copyedited and formatted. The final version may differ from this version.



reasons. Neurotrophin levels are reduced in many neurodegenerative diseases but are still detectable. Therefore, a therapy that allows these lower levels of endogenous neurotrophins to have a neuroprotective function would avoid the side effects of generalized neurotrophin therapy, which include thermal hyperalgesia, weight loss, and pain sensitivity.

Both PI-3Kinase and MAPKinase signaling downstream of TrkA are involved in the neurotrophic effects of NGF. The PI-3Kinase signaling pathway contributes more than MAPKinase pathway in neuronal survival (Kaplan and Miller, 2000; Shimoke and Chiba, 2001; Culmsee et al., 2002; Huang and Reichardt, 2003). The MAPKinase pathway, on the other hand, is essential for NGF-induced neurogenesis (Xiao and Liu, 2003). This may explain why 5E5 was better at stimulating differentiation than promoting survival, because 5E5 is a potent activator of ERK but a weaker activator of Akt. A low dose of 5E5 (3-10 μM) activates ERK as strongly as maximal dose of NGF (100 ng/ml), and 5E5 and NGF have additive effects on ERK (Supporting information 5). However, equivalent doses of 5E5 activate Akt weakly and, more importantly, impair NGF activation of Akt when given together (Supporting information 5). This likely explains the inability of 10 μM 5E5 to protect differentiated PC12 cell from apoptosis induced by NGF and serum withdrawal. We were unable to test higher concentrations of 5E5 in this assay due to cytotoxicity.

In summary, by screening asterriquinone and mono-indolyl-quinone libraries we were able to identify small molecule activators of TrkA, the NGF receptor. These



Downloaded from jpet.aspetjournals.org at ASPET Journals on April 16, 2024

JPET Fast Forward. Published on April 27, 2007 as DOI: 10.1124/jpet.106.118034
This article has not been copyedited and formatted. The final version may differ from this version.



compounds activate TrkA directly in cells and protect differentiated PC12 cells from apoptosis or promote neuronal differentiation. The QSAR models that we have constructed will guide further optimization of these compounds to maximize activator activity and minimize toxicity. Although 1H5 and 5E5 themselves are still unsuitable as drug candidates, they provide lead compounds that can be put into preclinical models of neurodegeneration for proof-of-principle experiments.

Downloaded from jpet.aspetjournals.org at ASPET Journals on April 16, 2024

JPET Fast Forward. Published on April 27, 2007 as DOI: 10.1124/jpet.106.118034
This article has not been copyedited and formatted. The final version may differ from this version.



## Acknowledgments:

We wish to thank Dr. Mobley (Stanford University) for the kind gift of PC12-TrkA (clone624) cells and Dr. Kaplan (University of Toronto) for the kind gift of NIH3T3-TrkA, TrkB and TrkC cells.

Downloaded from jpet.aspetjournals.org at ASPET Journals on April 16, 2024

JPET Fast Forward. Published on April 27, 2007 as DOI: 10.1124/jpet.106.118034
This article has not been copyedited and formatted. The final version may differ from this version.



## References:

Air EL, Strowski MZ, Benoit SC, Conarello SL, Salituro GM, Guan XM, Liu K, Woods SC, Zhang BB (2002) Small molecule insulin mimetics reduce food intake and body weight and prevent development of obesity. Nat. Med. 8:179-183.

Bibel M, Barde YA (2000) Neurotrophins: key regulators of cell fate and cell shape in the vertebrate nervous system. Genes Dev. 14:2919-2937.

Bothwell M (1995) Functional interactions of neurotrophins and neurotrophin receptors. Ann. Rev. Neuro. 18:223-253.

Chen XQ, Fawcett JR, Rahman YE, Ala TA, Frey II WH (1998) Delivery of NGF to the Brain via the Olfactory Pathway. J. Alz. Dis. 1:35-44.

Culmsee C, Gerling N, Lehmann M, Nikolova-Karakashian M, Prehn JH, Mattson MP, Krieglstein J (2002) Nerve growth factor survival signaling in cultured hippocampal neurons is mediated through TrkA and requires the common neurotrophin receptor P75. Neuroscience. 115:1089-1108.

Dago L, Bonde C, Peters D, Moller A, Bomholt SF, Hartz JB, Meyer M, Drejer J, Gronborg M. (2002) NS 1231, a novel compound with neurotrophic-like effects in vitro



Downloaded from jpet.aspetjournals.org at ASPET Journals on April 16, 2024

JPET Fast Forward. Published on April 27, 2007 as DOI: 10.1124/jpet.106.118034
This article has not been copyedited and formatted. The final version may differ from this version.



and in vivo. J. Neurochem. 81:7-24.

Dechant G., Barde YA (2002) The neurotrophin receptor p75(NTR): novel functions and implications for diseases of the nervous system. Nat. Neurosci. 5:1131- 1136.

Friedman WJ, Greene LA (1999) Neurotrophin signaling via Trks and p75. Exp. Cell Res. 253:131-142.

Friedman WJ (2000) Neurotrophins induce death of hippocampal neurons via the p75NTR. J. Neurosci. 20:6340-6346.

Gronborg M, Johansen TE, Peters D, Ahring PK, Drejer J,Moller A, Jensen LH. (1999) Neuroprotection by a novel compound, NS 521. J. Pharmacol. Exp. Ther. 81:348-353.

Horner PJ, Gage FH (2000) Regenerating the damaged central nervous system. Nature 407: 963-970.

Huang EJ, Reichardt LF (2001) Neurotrophins: roles in neuronal development and function. Annu. Rev. Neurosci. 24:677-736.

Downloaded from jpet.aspetjournals.org at ASPET Journals on April 16, 2024

JPET Fast Forward. Published on April 27, 2007 as DOI: 10.1124/jpet.106.118034
This article has not been copyedited and formatted. The final version may differ from this version.



Huang EJ, Reichardt LF (2003) Trk receptors: roles in neuronal signal transduction. Annu. Rev. Biochem. 72:609-642.

Kaplan DR, Miller FD (2000) Neurotrophin signal transduction in the nervous system. Curr. Opin. Neurobiol. 10:381-391.

Kovatcheva A, Buchbauer G., Golbraikh A, and Wolschann P (2003) QSAR Modeling of α-Campholenic Derivatives with Sandalwood Odor. J. Chem. Inf. Comput. Sci. 43: 259 – 266.

Lee FS, Chao MV (2001) Activation of Trk neurotrophin receptors in the absence of neurotrophins. Proc Natl Acad Sci U S A. 98:3555-3560.

Liu K, Xu L, Szalkowski D, Li Z, Ding V, Kwei G, Huskey S, Moller DE, Heck JV, Zhang BB, Jones AB (2000) Discovery of a potent, highly selective, and orally efficacious small-molecule activator of the insulin receptor. J. Med. Chem. 43:3487-3494.

McMahon SB, Priestly JV (1995) Peripheral neuropathies and neurotrophic factors: animal models and clinical perspectives. Curr. Opin. Neurobiol. 5: 616-614.

Miller G. (2002) Drug targeting. Breaking down barriers. Science. 297:1116-1118.



Downloaded from jpet.aspetjournals.org at ASPET Journals on April 16, 2024

JPET Fast Forward. Published on April 27, 2007 as DOI: 10.1124/jpet.106.118034
This article has not been copyedited and formatted. The final version may differ from this version.



Morooka T, Nishida E (1998) Requirement of p38 Mitogen-activated Protein Kinase for Neuronal Differentiation in PC12 Cells. J. Biol. Chem. 273: 24285-24288.

Patapoutian A, Reichardt LF (2001) Trk receptors: mediators of neurotrophin action. Curr. Opin. Neurobiol. 11:272-280.

[a] Pirrung MC, Liu Y, Deng L, Halstead DK, Li Z, May JF, Wedel M, Austin DA, Webster NJ (2005) Methyl scanning: total synthesis of demethylasterriquinone B1 and derivatives for identification of sites of interaction with and isolation of its receptor(s). J. Am. Chem. Soc. 127:4609-4624.

[b]Pirrung MC, Fujita K, Park K (2005) Organometallic routes to 2,5-dihydroxy-3-(indol-3-yl)benzoquinones. Synthesis of demethylasterriquinone B4. J. Org. Chem. 70:2537-2542.

Poo MM (2001) Neurotrophins as synaptic modulators. Nat. Rev. Neurosci. 2,24-32.

Saragovi HU, Gehring K (2000) Development of pharmacological agents for targeting neurotrophins and their receptors. Trends Pharmacol. Sci. 21:93–98.

Downloaded from jpet.aspetjournals.org at ASPET Journals on April 16, 2024

JPET Fast Forward. Published on April 27, 2007 as DOI: 10.1124/jpet.106.118034
This article has not been copyedited and formatted. The final version may differ from this version.



Schmidt CE, Shastri VR, Vacanti JP, Langer R (1997) Stimulation of neurite outgrowth using an electrically conducting polymer. Proc. Natl. Acad. Sci. USA. 94: 8948–8953.

Shimoke K, Chiba H (2001) Nerve growth factor prevents 1-methyl-4-phenyl-1,2,3,6-tetrahydropyridine-induced cell death via the Akt pathway by suppressing caspase-3-like activity using PC12 cells: relevance to therapeutical application for Parkinson's disease. J. Neurosci. Res. 63:402-409.

Sivananthan S, Leavitt B (2005) Got NGF? Promising gene therapy results in Alzheimer's disease. Clin. Genet. 68,194-196.

Thoenen H (2000) Neurotrophins and activity-dependent plasticity. Prog. Brain Res. 128:183-191.

Thorne RG., Frey WH 2nd (2001) Delivery of neurotrophic factors to the central nervous system: pharmacokinetic considerations. Clin. Pharmacokinet. 40:907-946.

Troy CM, Friedman JE, Friedman WJ (2002) Mechanisms of p75-mediated death of hippocampal neurons. Role of caspases. J. Biol. Chem. 277:34295-34302.

Tuszynski MH, Thal L, U HS, Pay MM, Blesch A, Conner J, Vahlsing HL (2002) NGF



Downloaded from jpet.aspetjournals.org at ASPET Journals on April 16, 2024

JPET Fast Forward. Published on April 27, 2007 as DOI: 10.1124/jpet.106.118034
This article has not been copyedited and formatted. The final version may differ from this version.



gene therapy for Alzheimer's disease. J. Mol. Neurosci. 19:207-208.

Tuszynski MH, Thal L, Pay M, Salmon DP, U HS, Bakay R, Patel P, Blesch A, Vahlsing HL, Ho G, Tong G, Potkin SG, Fallon J, Hansen L, Mufson EJ, Kordower JH, Gall C, Conner J (2005) A phase 1 clinical trial of nerve growth factor gene therapy for Alzheimer disease. Nat. Med. 11:551-555.

Wilkie N, Wingrove PB, Bilsland JG, Young L, Harper SJ, Hefti F, Ellis S, Pollack SJ (2001) The non-peptidyl fungal metabolite L-783,281 activates TRK neurotrophin receptors. J. Neurochem. 78:1135-1145.

Winkler J, Thal LJ, Gage FH, Fisher LJ (1998) Cholinergic strategies for Alzheimer's disease. J. Mol. Med. 76:555-567.

Xiao J, Liu Y (2003) Differential roles of ERK and JNK in early and late stages of neuritogenesis: a study in a novel PC12 model system. J. Neurochem. 86:1516-1523.

Zhang B, Salituro G, Szalkowski D, Li Z, Zhang Y, Royo I, Vilella D, Diez MT, Pelaez F, Ruby C, Kendall RL, Mao X, Griffin P, Calaycay J, Zierath JR, Heck JV, Smith RG, Moller DE (1999) Discovery of a small molecule insulin mimetic with antidiabetic activity in mice. Science. 284:974-977.



Downloaded from jpet.aspetjournals.org at ASPET Journals on April 16, 2024

JPET Fast Forward. Published on April 27, 2007 as DOI: 10.1124/jpet.106.118034
This article has not been copyedited and formatted. The final version may differ from this version.



## Footnotes:

This study was supported by grants from the American Diabetes Association (M.C.P) and the National Institute for Aging (N.J.G.W) (RO3 AG023191). N.J.G.W. is a faculty member of the UCSD Biomedical Sciences Graduate Program.

Address correspondence to: Nicholas J.G. Webster, Ph.D. Stein Clinical Research Bldg. 201, Department of Medicine (0673), University of California, San Diego, 9500 Gilman Drive, La Jolla, CA 92093-0673.

Tel: (858) 534-6275, FAX: (858) 534-6653, E-mail:nwebster@ucsd.edu

## Supporting information available:

1.The structure vs. activity and cell viability of asterriquinone library.

2. The structure vs. activity and cell viability of mono-indolyl-quinone library.

3. The neural net dependency plots for TrkA activity by both asterriquinone library and mono-indolyl-quinone library.

4. Summary of linear regression models showing coefficient, partial F value, and t-probability for most important variables.

5. The additive effects of 5E5 on NGF activation of TrkA, ERK and Akt.

Downloaded from jpet.aspetjournals.org at ASPET Journals on April 16, 2024

JPET Fast Forward. Published on April 27, 2007 as DOI: 10.1124/jpet.106.118034
This article has not been copyedited and formatted. The final version may differ from this version.



## Legends for Figures:

**Legends for Supporting Information: 1.**Table shows the structure vs. TrkA activity and cell viability for the asterriquinone library. Activity is expressed as percent of 100 ng/ml NGF; cell viability is expressed as percent of vehicle treated cells.

**2.** Table shows the structure vs. activity and cell viability of mono-indolyl-quinone library. Activity is expressed as percent of 100 ng/ml NGF; cell viability is expressed as percent of vehicle treated cells.

**3.** The neural net dependency plots for TrkA activity derived from QSAR studies with the asterriquinone library (panel A) or the mono-indolyl-quinone library (panel B). Substituent parameters were systematically varied and the resulting change in predicted output determined.

**4.** Summary of linear regression models. Tables show regression models for TrkA activity and cell viability for the asterriquinone or monoquinone libraries. Each table shows the parameter, its coefficient, partial F value, and t-probability for the most important variables.

**5.** Starved PC12-TrkA cells were stimulated with different doses of 5E5 (0 μM, 3 μM, 30μM) plus different doses of NGF (0 ng/ml, 10 ng/ml, 30 ng/ml, 100 ng/ml) for 10 min, lysed and immunoblotted with anti-phospho-TrkA (Tyr490), anti-phospho-ERK (Tyr204), anti-phospho-Akt (Ser473). Top panel: 5E5 has additive effects on TrkA activation of NGF. Middle panel: 5E5 can enhance NGF activation on ERK. Bottom panel: 5E5 can impair NGF activation on Akt.



Downloaded from jpet.aspetjournals.org at ASPET Journals on April 16, 2024

JPET Fast Forward. Published on April 27, 2007 as DOI: 10.1124/jpet.106.118034
This article has not been copyedited and formatted. The final version may differ from this version.



**Fig. 1:** Structure of the asterriquinone. Panel A: Structure of the lead compound demethylasterriquinone-B1 (DAQ-B1). Panel B: Retro-synthetic analysis demonstrating combinatorial approach.

**Fig. 2:** QSAR models for TrkA activation by both asterriquinone and mono-indolyl-quinone libraries. Compounds were used at 30 μM for the library screen. Panel A: Generic structure of the asterriquinone library. Panel B: Forward feed neural net model for TrkA activation by the asterriquinone library. Neural network was trained using a set of 188 exploratory variables with TrkA activation measured by ELISA as the target variable. Final model was obtained after 3482 cycles. Panel C: Multiple linear regression model for TrkA activation by the asterriquinone library using 188 exploratory variables. Panel D: Schematic of results from modeling of asterriquinone data. Panel E: Generic structure of the mono-indolyl-quinone library. Panel F: Forward feed neural net model for TrkA activation of mono-indolyl-quinone library. Neural network was trained using 45 exploratory variables. Final model was obtained after 1351 cycles. Panel G: Multiple linear regression model for TrkA activation by the mono-indolyl-quinone library using the 45 exploratory variables. Panel H: Schematic of results from modeling of monoquinone data. In panels B, C, F, and G the actual values are shown on x-axis, predicted values on y-axis. Activity is relative to 100 ng/ml NGF. In panels D and H, lower right semicircles depict results from forward feed neural nets, upper left semicircles depict results from multiple linear regression. Black indicates a positive

Downloaded from jpet.aspetjournals.org at ASPET Journals on April 16, 2024

JPET Fast Forward. Published on April 27, 2007 as DOI: 10.1124/jpet.106.118034
This article has not been copyedited and formatted. The final version may differ from this version.



correlation with the substituent parameter and grey indicates a negative correlation.

**Fig. 3:** Lack of correlation of cytotoxicity and TrkA activation. Panel A: Scatter plot of $IC_{50}$ for cytotoxicity vs. TrkA activation. Panel B: Scatter plot of cell viability at 100 μM compound vs. TrkA activation. No correlation was observed between cytotoxicity and TrkA activation demonstrating that the toxicity is not activity dependent. Panel C: Forward feed neural net model for toxicity of the asterriquinone library using 188 exploratory variables. Final model was obtained after 2573 cycles. Panel D: Multiple linear regression model for toxicity of the asterriquinone library using 188 variables. Panel E: Forward feed neural net model for toxicity of the mono-indolyl-quinone library using 45 exploratory variables. Final model was obtained after 849 cycles. Panel F: Multiple linear regression model for toxicity of the mono-indolyl-quinone library using 45 variables. In panels C – F, actual values are shown on x-axis, predicted values on y-axis. Activity is relative to 100 ng/ml NGF; cell viability is relative to untreated cells. Panels G and H: Schematic of results from modeling of asterriquinone and monoquinone cell viability data, respectively. Lower right semicircles depict results from forward feed neural nets, upper left semicircles depict results from multiple linear regression. Black indicates a positive correlation with the substituent parameter and grey indicates a negative correlation.

**Fig. 4:** Characterization of the two activators chosen for further study. Panel A: Structures of compound 1H5 and 5E5. Panel B: Molecular modeling of asterriquinone



Downloaded from jpet.aspetjournals.org at ASPET Journals on April 16, 2024

JPET Fast Forward. Published on April 27, 2007 as DOI: 10.1124/jpet.106.118034
This article has not been copyedited and formatted. The final version may differ from this version.



1H5 that contains a cyclopropyl group at the C-2 position of one indole and a chlorine substitution on the other indole. The dihedral angles are $97^{o}$ and $145^{o}$ respectively. Panel C: Molecular modeling of mono-indolyl-quinone 5E5 that contains 2,5 dimethoxy substitutions on the quinone. The methoxy group causes a predicted dihedral angle of $74^{o}$ due to steric hindrance. Molecular mechanical simulations were performed with CORINA and then 3D structures optimized with COSMIC. Carbon atoms are shown in gray, hydrogen in white, oxygen in red, nitrogen in blue, chlorin in green, and fluorine in yellow. Space filling representatives are shown. Panel D: Comparison of TrkA activation by 30 μM 1H5, 5E5 and DAQ-B1 in CHO-TrkA cells. Data are mean ± S.E. of six experiments and are presented as percent activity relative to the 100 ng/ml NGF. Panel E: Dose-dependent cytotoxicity of 1H5, 5E5 and DAQ-B1 on CHO-TrkA cells. Data are mean ± S.D. of duplicate experiments and are presented as percentage of control cells without treatment. Asterisks indicate statistical significance relative to untreated control (*, $p<0.05$; **, $p < 0.01$; ***, $p<0.001$).

**Fig. 5:** Asterriquinones 1H5 can protect differentiated PC12 neurons from apoptosis induced by NGF and serum withdrawal. Panel A: Effect of compounds 1H5 on TrkA signaling. Starved PC12-TrkA cells were stimulated with 1H5 or NGF for 10 min, lysed and immunoblotted with anti-phospho-TrkA (Tyr490), anti-phospho-Akt (Ser473), anti-phospho-ERK (Tyr204). Representative blots are shown, and blots were quantified with Image J and normalized to total ERK1/2 as a loading control. Data are mean±S.D. of triplicate experiments and are presented as percent activity relative to 100 ng/ml NGF.

Downloaded from jpet.aspetjournals.org at ASPET Journals on April 16, 2024

JPET Fast Forward. Published on April 27, 2007 as DOI: 10.1124/jpet.106.118034
This article has not been copyedited and formatted. The final version may differ from this version.



Panel B: PC12 cells were differentiated in complete medium for 7 days with 100 ng/ml NGF, and then changed to serum free F12K medium with 1H5 or NGF. The number of surviving cells was determined at 24 h, 48 h, 72 h using the MTS CellTiter assay in triplicate wells and are presented as percentage of positive control cells treated with 100 ng/ml NGF and serum. Asterisks indicate statistical significance relative to serum free F12K medium (SFM) only (*, $p < 0.05$; **, $p < 0.01$). Data are the means ± S.E. from six independent experiments. Panel C: Representative photos of cells after 72 h of serum and NGF withdrawal. Most cells in serum free medium (SFM) show apoptotic figures. Treatment with activator 1H5 preserves the morphology of the cell bodies and prevents apoptotic figures, but does not prevent regression of the neurites on the cells. NGF preserved neurite morphology. (Magnification x200.).

**Fig. 6:** Effect of compound 5E5 on TrkA signaling. Panels A, B, C and D: Starved PC12-TrkA cells were stimulated with increasing doses of 5E5 (0.3, 1, 3, 10, 30, 100 μM) or NGF (100 ng/ml) for 10 min, lysed and immunoblotted with anti-phospho-TrkA (Tyr490)(Panel A), anti-phospho-TrkA (Tyr674/675)(Panel B), anti-phospho-ERK (Tyr204)(Panel C), anti-phospho-Akt (Ser473)(Panel D). Representative blots are shown, and blots were quantified with Image J, normalized to total ERK1/2 as a loading control. Data are mean±S.D. of triplicate experiments and are presented as percent activity relative to 100 ng/ml NGF treatment. Panel E: PC12-TrkA cells were stimulated with 5E5 (30 μM) or NGF (100 ng/ml) for 10 min, lysed and SNT/FRS1 was precipitated on $p13^{suc1}$ agarose beads. The resulting pellets were subjected to western blot analysis with



Downloaded from jpet.aspetjournals.org at ASPET Journals on April 16, 2024

JPET Fast Forward. Published on April 27, 2007 as DOI: 10.1124/jpet.106.118034
This article has not been copyedited and formatted. The final version may differ from this version.



PY20 antibody. Panel F: PC12-TrkA cells were left unstimulated (basal) or were treated with either NGF (100 ng/ml) or 5E5 (10 μM) for the time indicated. Cells were lysed and immunoblotted with the anti-phospho-TrkA (Tyr490). Panels G, H and I: NIH3T3-TrkA, TrkB, TrkC cells were stimulated with increasing doses of 5E5 or the corresponding neurotrophins. Cells were lysed and immunoblotted with anti-phospho-Trk (Tyr490). This antibody can recognize TrkA, TrkB and TrkC when they are phosphorylated at the equivalent site. Representative blots are shown, multiple blots were quantified with Image J. Data are mean±S.D. of triplicate or duplicate experiments and are presented as percent activity relative to maximum neurotrophin treatment (100 ng/ml NGF or BDNF or NT-3). Panel J: The effect of PP1 on 5E5 signaling. PC12-Trk cells were pretreated with PP1 (100 nM + or 1 μM ++) for 30 min, and then stimulated with 30 μM 5E5 or 100 ng/ml NGF for 10 min or with 100 μM adenosine for 2h. Cell extracts were blotted for phospho-TrkA (Tyr 490), then reblotted with TrkA. Panel K: CHO-IRβ cells were starved and stimulated with indicated treatments for 10 min, lysed and immunoblotted with anti-IR/IGF1R (pYpY1162/1163) and reblotted with anti-IRβ.

**Fig. 7:** The effect of 5E5 on neurite outgrowth of PC12 cells. Panel A: Effect of 5E5 on neurite bearing cells. PC12 cells were stimulated with 5E5 (1 μM), NGF (10, 100 ng/ml), 5E5 (1 μM) plus NGF (10 ng/ml) in complete medium for 4 days, with a change of medium every two days. Cells were considered to be neurite bearing when the neurite length was >1.5 fold of cell body diameter. In each instance, 8 random fields were scored for neurite outgrowth. Data are presented as percentage of neurite bearing



Downloaded from jpet.aspetjournals.org at ASPET Journals on April 16, 2024

JPET Fast Forward. Published on April 27, 2007 as DOI: 10.1124/jpet.106.118034
This article has not been copyedited and formatted. The final version may differ from this version.



cells among the total cells (mean ± S.D.). Asterisks indicate statistical significance relative to 10 ng/ml NGF only group (**, $p < 0.01$). Panel B: Effect of 5E5 on neurite length. The total length of neurites in the field was divided by the total number of cells, giving the average neurite length for each cell. The treatments are shown on x-axis, the average neurite length (μm) on y-axis (**, $p < 0.01$ vs. 10 ng/ml NGF alone). Panel C: The morphology of PC12 cell after different treatments. (Magnification x100.)

Downloaded from jpet.aspetjournals.org at ASPET Journals on April 16, 2024

# Fig.1

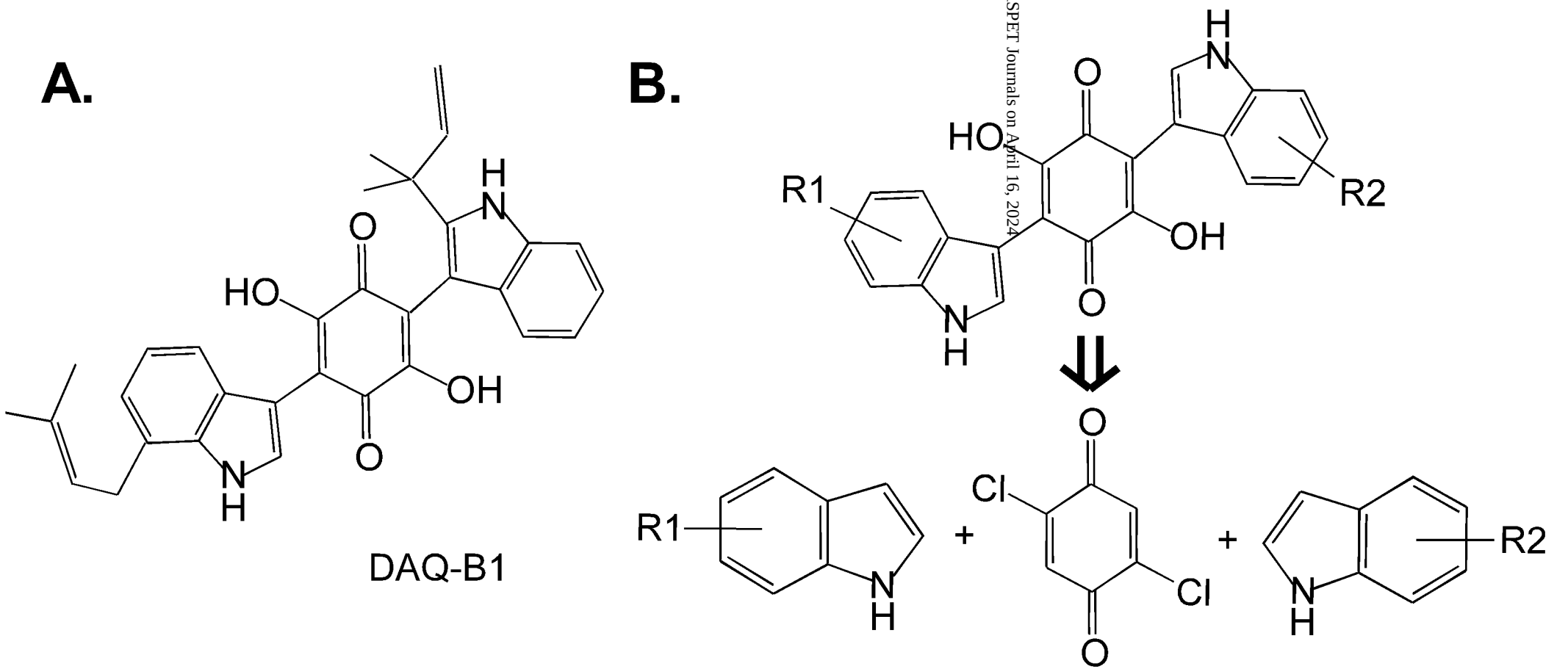


Downloaded from jpet.aspetjournals.org at ASPET Journals on April 16, 2024

# Fig.2

JPET Fast Forward. Published on April 27, 2007 as DOI: 10.1124/jpet.106.118034
This article has not been copyedited and formatted. The final version may differ from this version.

A.

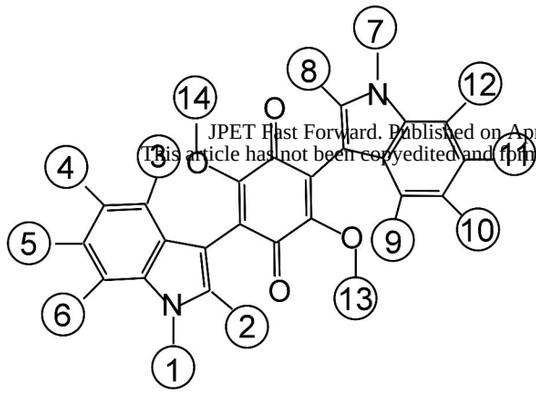


E.

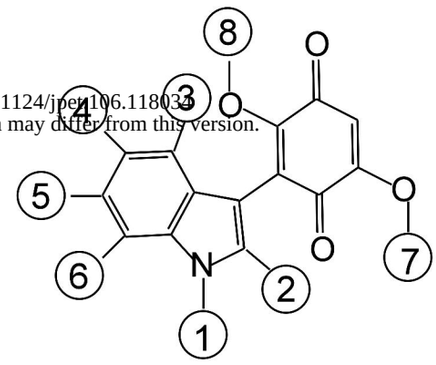


B.

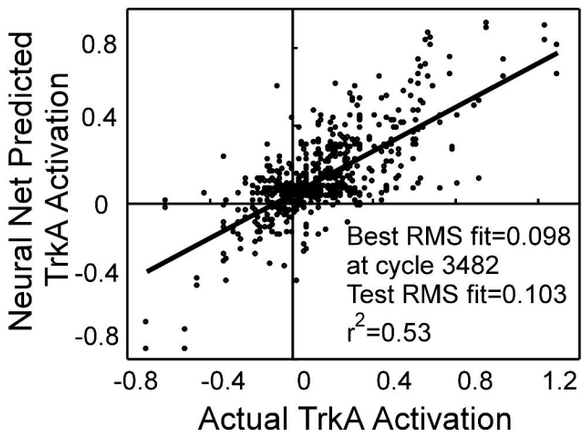


F.

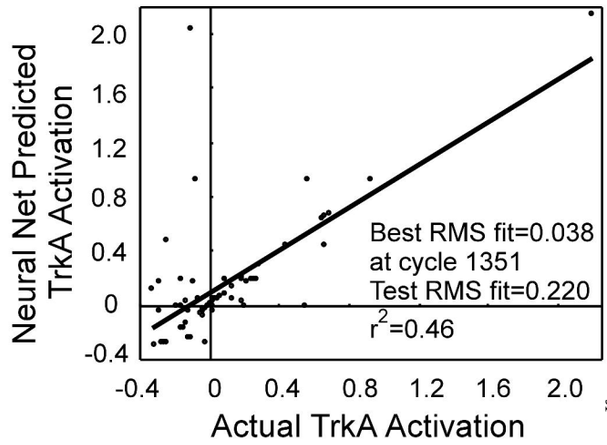


C.

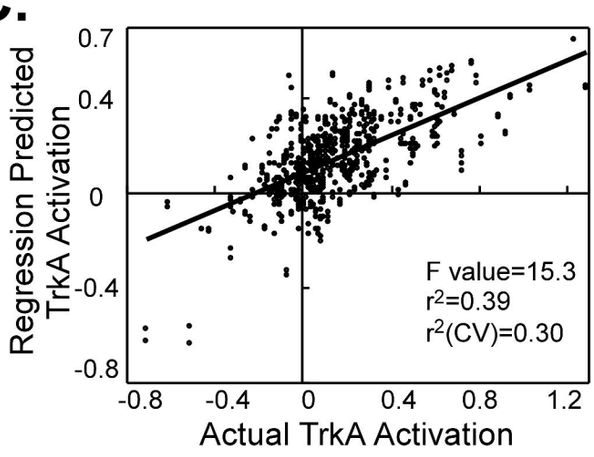


G.

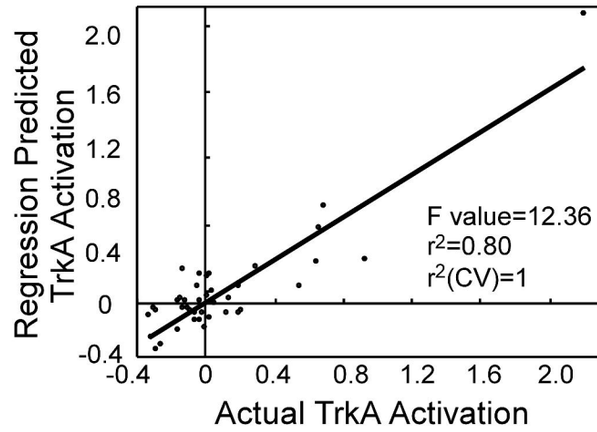


D.

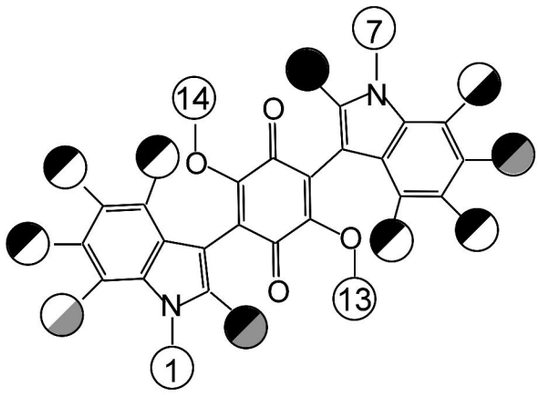


H.

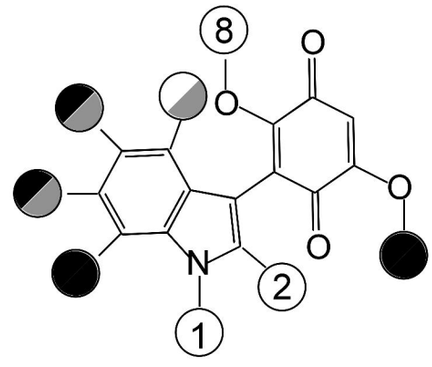


Downloaded from jpet.aspetjournals.org at ASPET Journals on April 16, 2024

# Fig.3

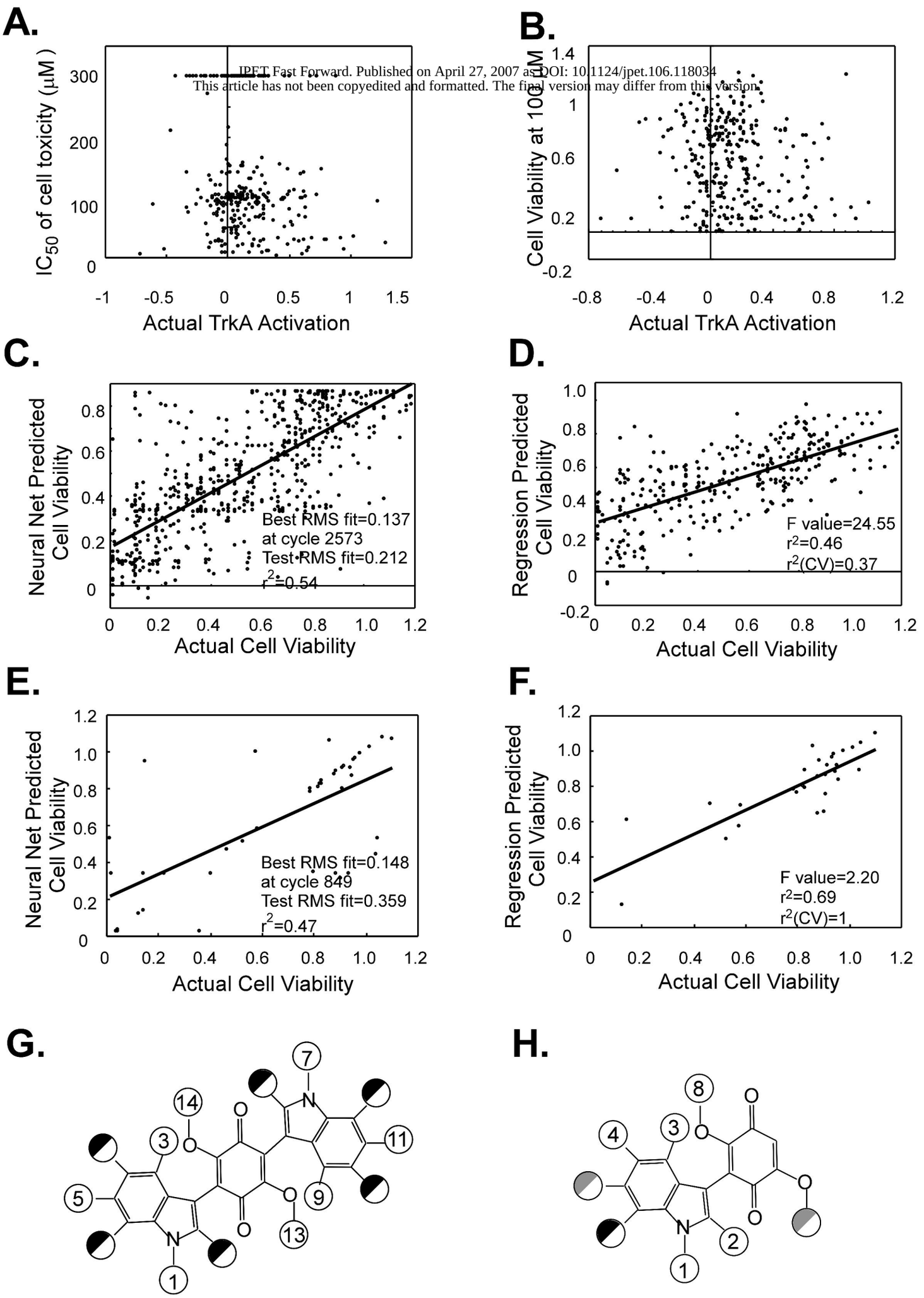


JPET Fast Forward. Published on April 27, 2007 as DOI: 10.1124/jpet.106.118034
This article has not been copyedited and formatted. The final version may differ from this version.

Downloaded from jpet.aspetjournals.org at ASPET Journals on April 16, 2024

# Fig.4

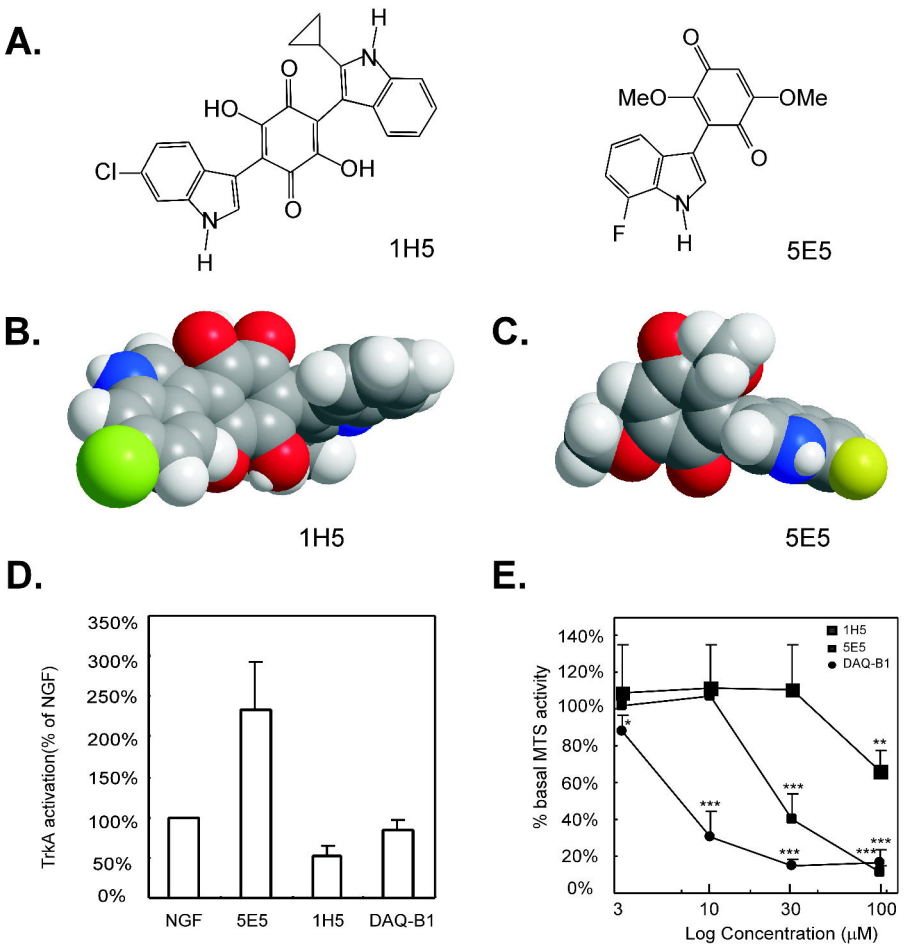
A.
H
N
O
HO
OH
Cl
O
N
H
1H5
O
MeO
OMe
O
N
F
H
5E5
B.
1H5
C.
5E5
D.
350%
300%
250%
200%
150%
100%
50%
0%
TrkA activation(% of NGF)
NGF
5E5
1H5
DAQ-B1
E.
140%
120%
100%
80%
60%
40%
20%
0%
% basal MTS activity
1H5
5E5
DAQ-B1
*
**
***
***
***
***
***
3
10
30
100
Log Concentration (μM)

# Fig.5

JPET Fast Forward. Published on April 27, 2007 as DOI: 10.1124/jpet.106.118034
This article has not been copyedited and formatted. The final version may differ from this version.

A.

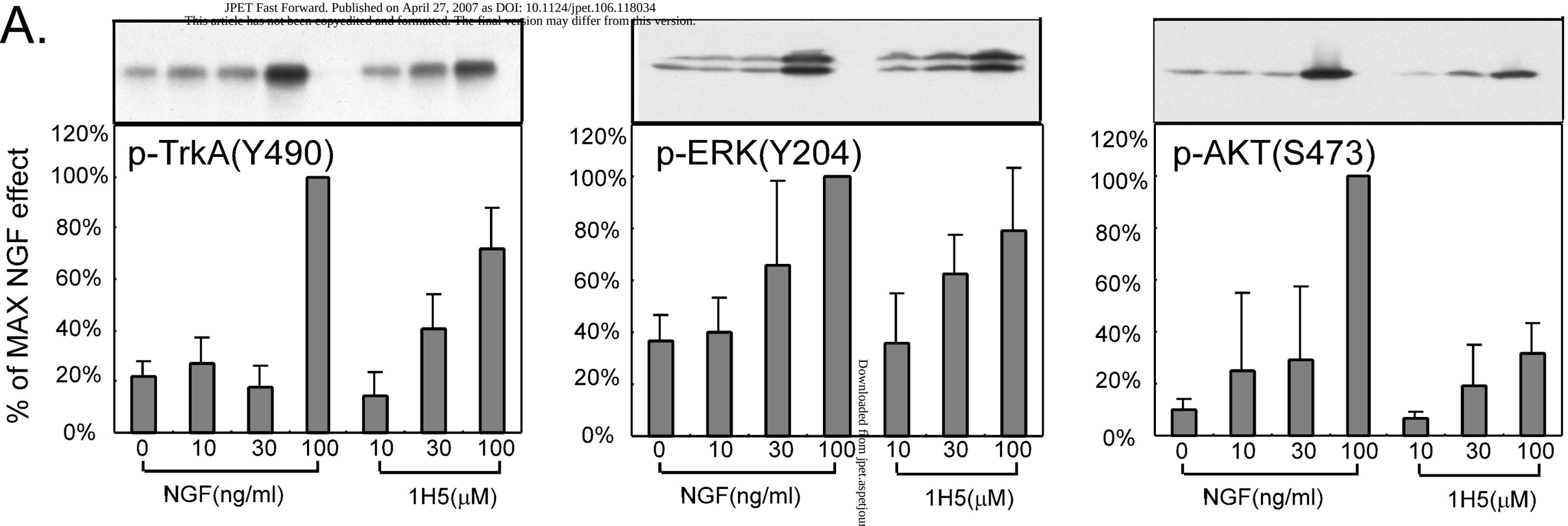


B.

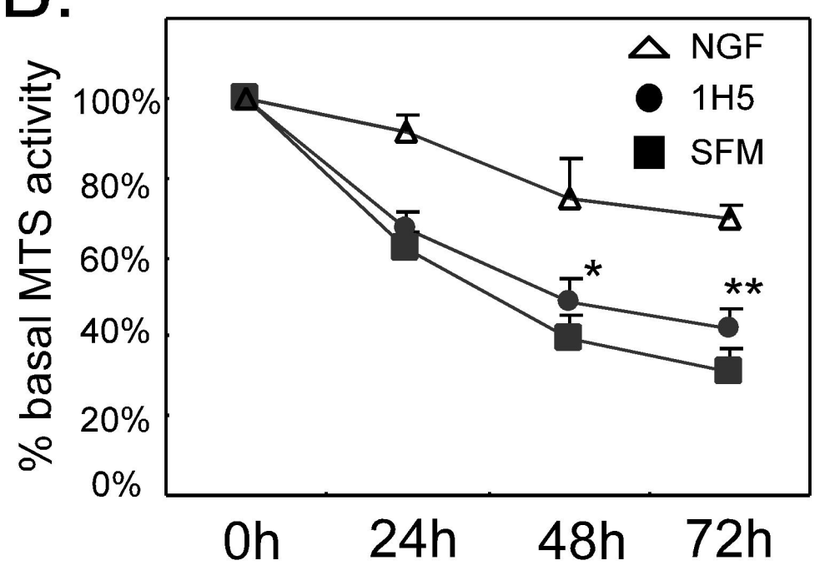


C.

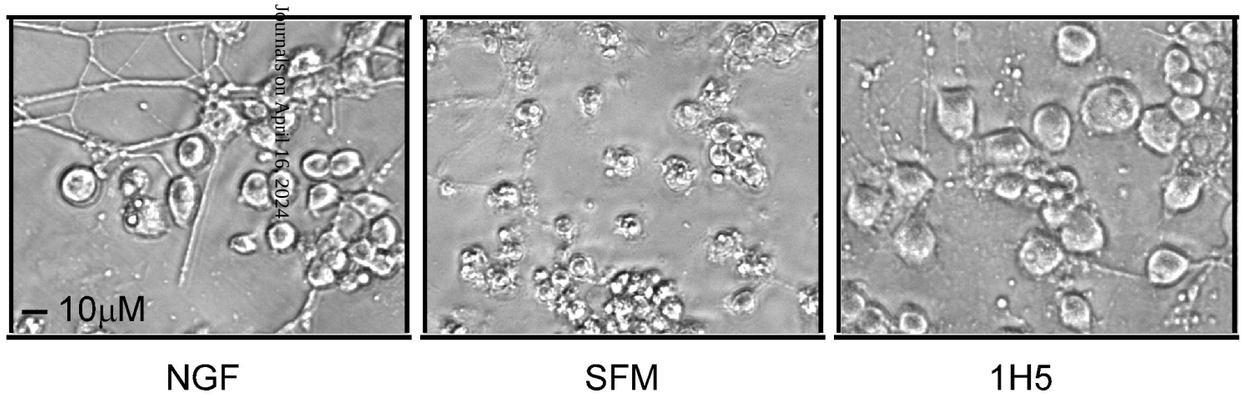


Downloaded from jpet.aspetjournals.org at ASPET Journals on April 16, 2024

# Fig.6

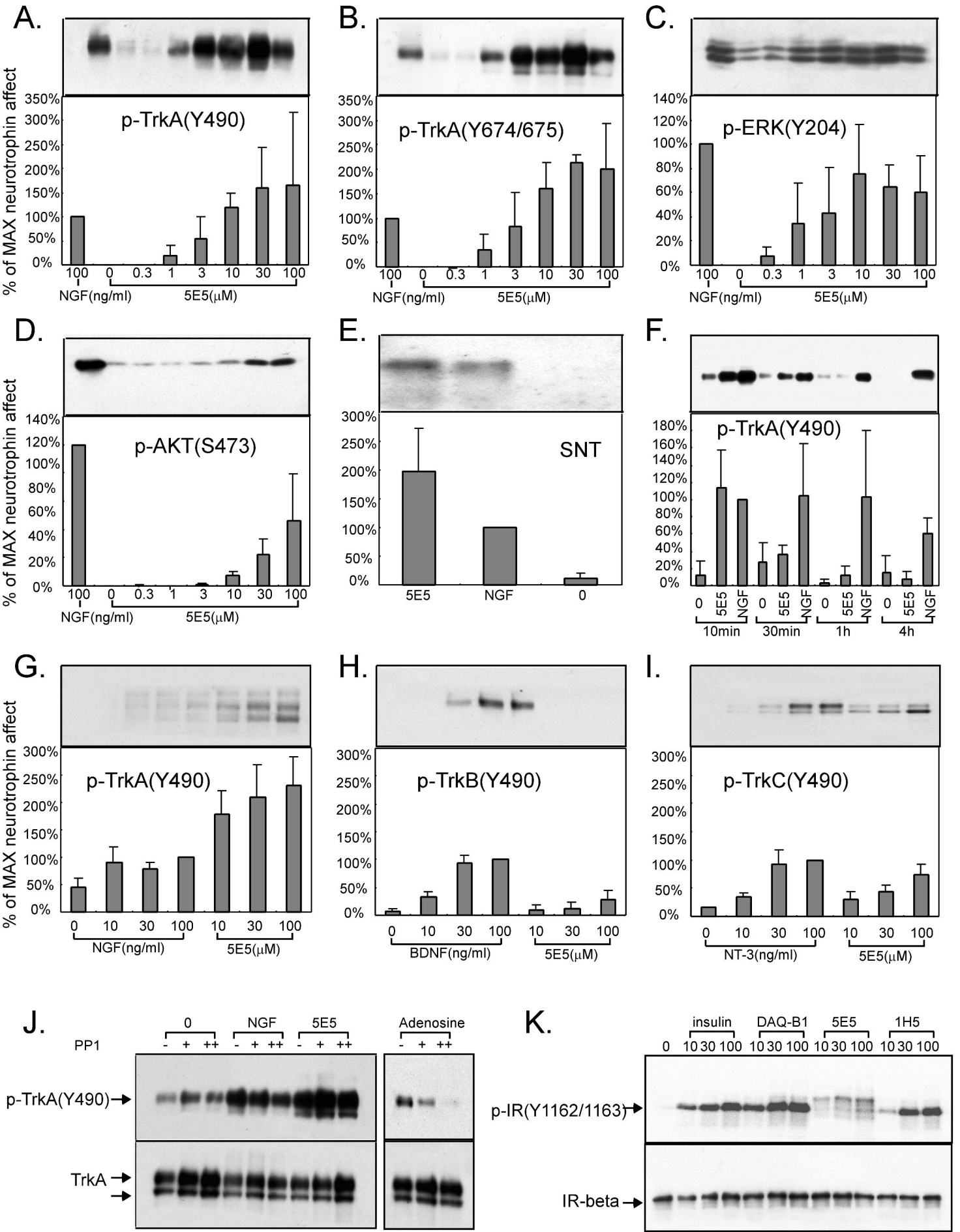
A.
p-TrkA(Y490)
% of MAX neurotrophin affect
NGF(ng/ml)
5E5(μM)
B.
p-TrkA(Y674/675)
C.
p-ERK(Y204)
D.
p-AKT(S473)
E.
SNT
5E5
NGF
F.
p-TrkA(Y490)
10min
30min
1h
4h
G.
p-TrkA(Y490)
H.
p-TrkB(Y490)
BDNF(ng/ml)
I.
p-TrkC(Y490)
NT-3(ng/ml)
J.
PP1
0
NGF
5E5
Adenosine
p-TrkA(Y490)
TrkA
K.
insulin
DAQ-B1
5E5
1H5
p-IR(Y1162/1163)
IR-beta

# Fig.7

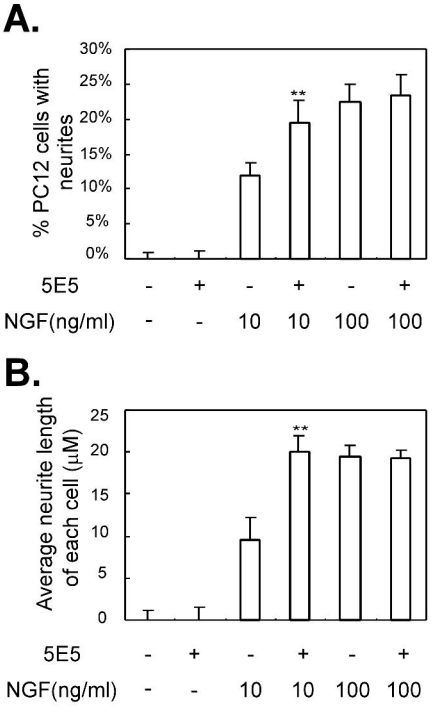
A.
% PC12 cells with neurites
30%
25%
20%
15%
10%
5%
0%
**
5E5 - + - + - +
NGF(ng/ml) - - 10 10 100 100
B.
Average neurite length of each cell (μM)
25
20
15
10
5
0
**
5E5 - + - + - +
NGF(ng/ml) - - 10 10 100 100
C.
0
5E5
NGF10 ng/ml
NGF10 ng/ml + 5E5
NGF100 ng/ml
NGF100 ng/ml + 5E5
20μM